

Forcing Mechanisms of the Interannual Sea Level Variability in the Midlatitude South Pacific during 2004–2020

C. Germeaud ^{1,2,3,4,*}, D. L. Volkov ^{1,2}, S. Cravatte ³ and W. Llovel ⁵

¹ Cooperative Institute for Marine and Atmospheric Studies, University of Miami, Miami, FL 33149, USA

² NOAA, Atlantic Oceanographic and Meteorological Laboratory, Physical Oceanography Division, Miami, FL 33149, USA

³ LEGOS, Université de Toulouse, CNES, CNRS, IRD, UPS, 31400 Toulouse, France

⁴ Centre National d'Études Spatiales, 31401 Toulouse, France

⁵ LOPS, CNRS, University of Brest, IFREMER, IRD, 29238 Plouzané, France

* Correspondence: cyril.germeaud@cnes.fr

Figures:

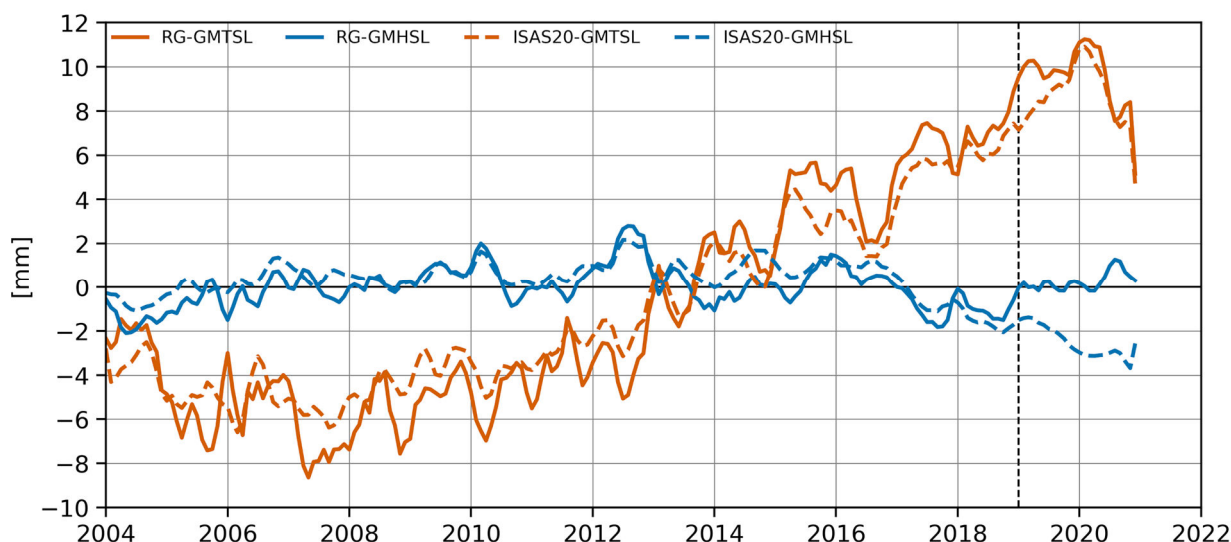


Figure S1. Time series of the global mean thermosteric sea level (GMTSL; orange curves) and halosteric sea level (GMHSL; blue curves) anomalies relative to the 2006–2015 mean (as in Barnoud et al., 2021) for the 2004–2020 period and derived from two Argo-based products: (i) the Roemmich-Gilson (RG) Climatology (solid curves) and (ii) the 8th version of the In Situ Analysis System, ISAS20 (dashed curves). For each time series, the monthly mean climatology was removed and a 3-month low-pass filter was applied to remove remaining subseasonal signals. The dominant influence of the Argo “salty drift” (<https://argo.ucsd.edu/data/data-faq/#sbepsal>; last access on 2 January 2023) on ISAS20 salinity data is seen in 2019 (dashed vertical line) and onwards due to the lack of delayed-mode adjusted salinity profiles.

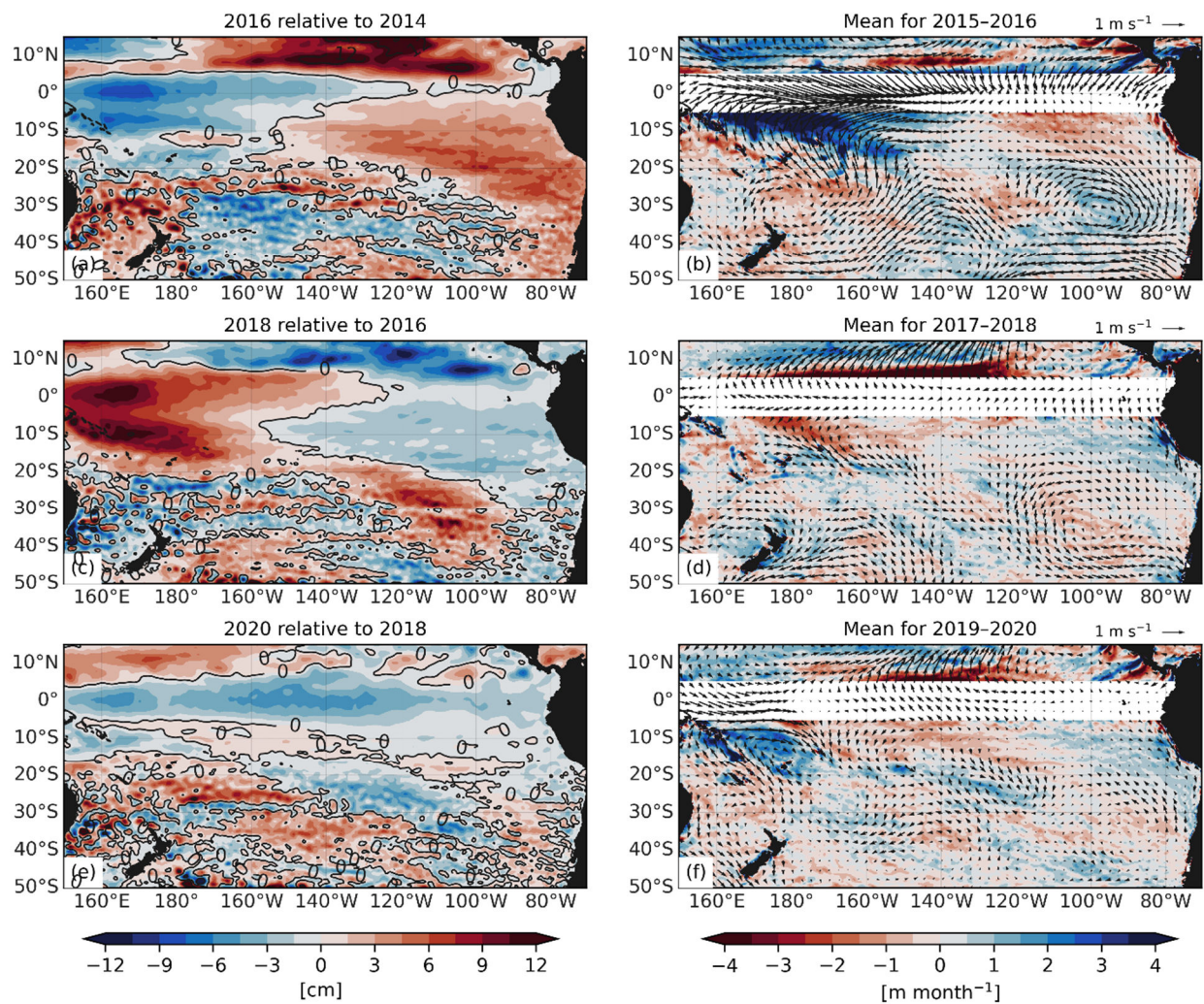


Figure S2. As in Figure 2, differences in sea level anomaly (SLA) derived from satellite altimetry for 2016 minus 2014 in (a) 2018 minus 2016 in (c) and 2020 minus 2018 in (e). Ekman pumping anomalies W_{Ek} (color; positive upward) with respect to the 1993–2020 time mean and averaged over (b) 2015–2016, (d) 2017–2018 and (f) 2019–2020 instead of the Ekman solution shown in Figure 2. W_{Ek} values over 5°S–5°N are excluded (as the Coriolis parameter tends towards zero near the equator) and the corresponding 10-m wind velocity anomalies are also shown (arrows).

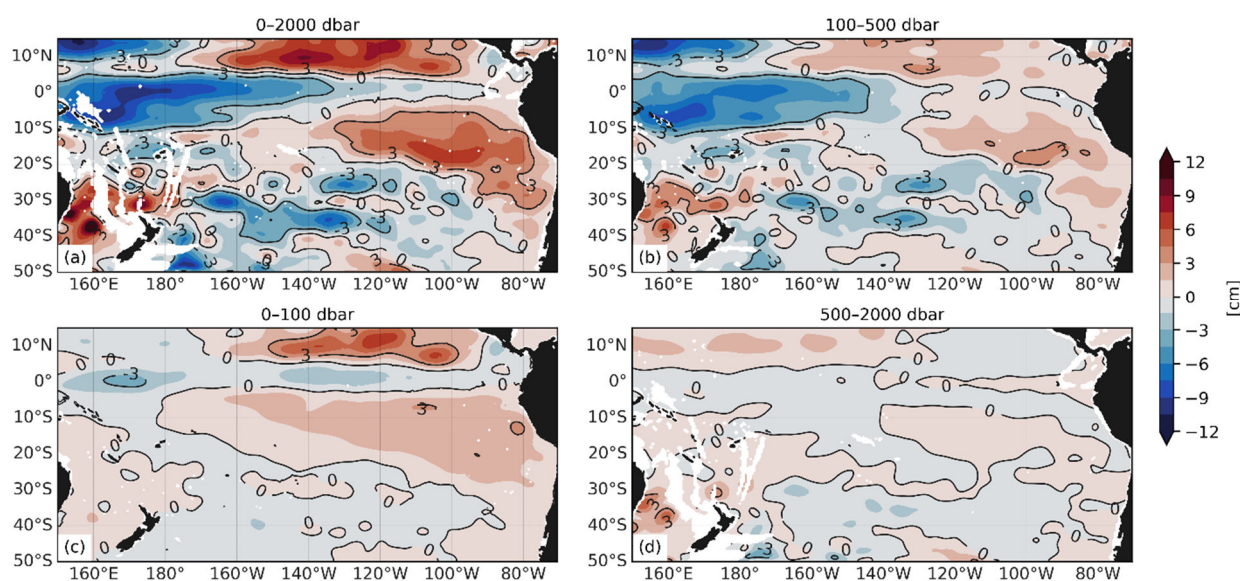


Figure S3. Differences in the 8th version of the In Situ Analysis System (ISAS20) Argo-based thermosteric sea level (TSL) for 2016 minus 2014 over (a) 0–2000 dbar, (b) 100–500 dbar, (c) 0–100 dbar and (d) 500–2000 dbar. Contour lines (see inline numbers for TSL intervals) are also shown. In each panel, white shading indicates areas where bathymetry is shallower than each pressure reference level.

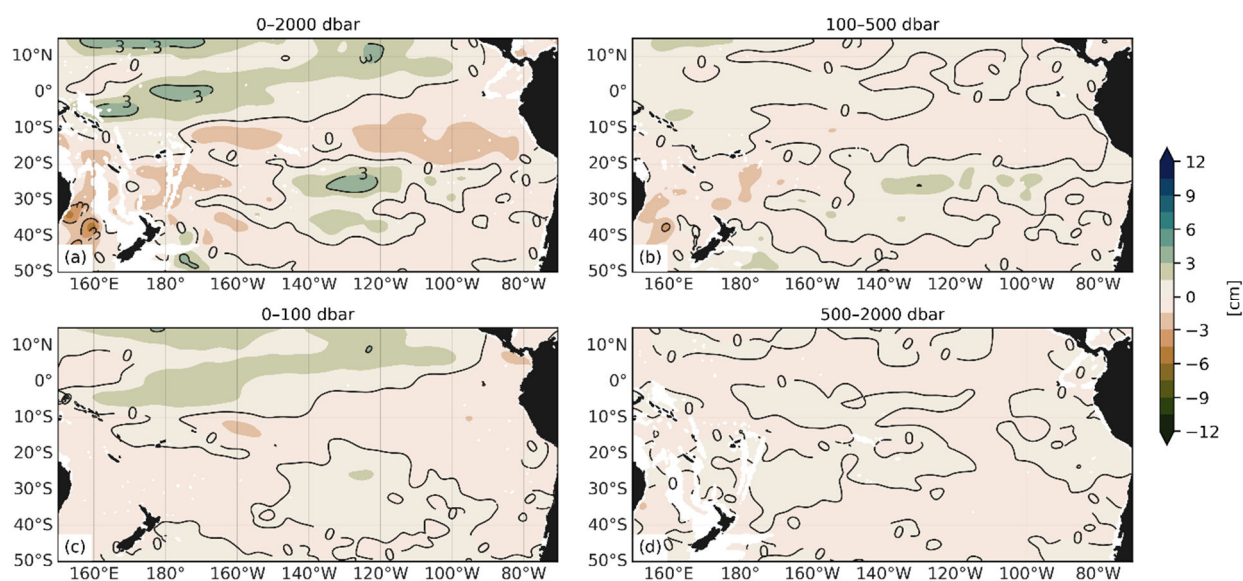


Figure S4. Differences in the 8th version of the In Situ Analysis System (ISAS20) Argo-based halosteric sea level (HSL) for 2016 minus 2014 over (a) 0–2000 dbar, (b) 100–500 dbar, (c) 0–100 dbar and (d) 500–2000 dbar. Contour lines (see inline numbers for HSL intervals) are also shown. In each panel, white shading indicates areas where bathymetry is shallower than each pressure reference level.

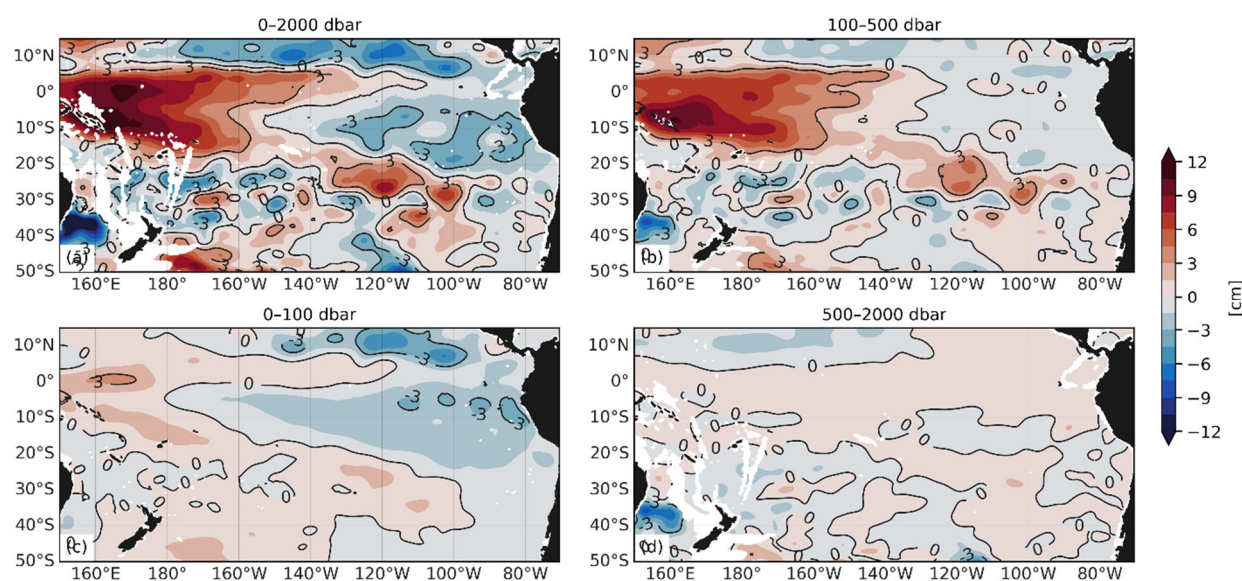


Figure S5. Differences in the 8th version of the In Situ Analysis System (ISAS20) Argo-based thermosteric sea level (TSL) for 2018 minus 2016 over (a) 0–2000 dbar, (b) 100–500 dbar, (c) 0–100 dbar and (d) 500–2000 dbar. Contour lines (see inline numbers for TSL intervals) are also shown. In each panel, white shading indicates areas where bathymetry is shallower than each pressure reference level.

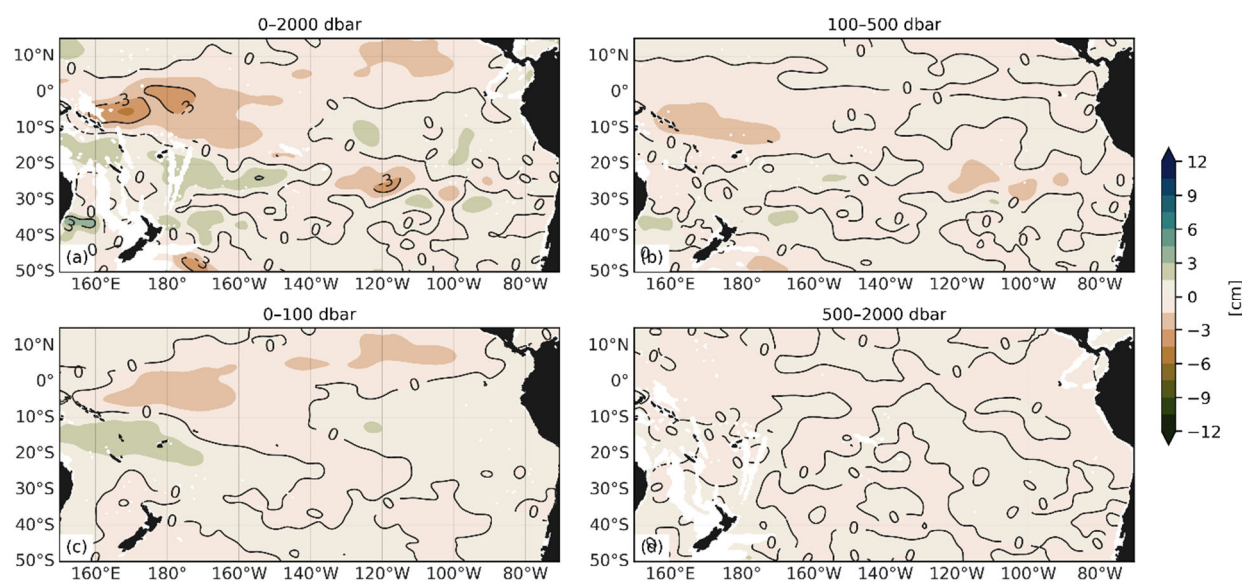


Figure S6. Differences in the 8th version of the In Situ Analysis System (ISAS20) Argo-based halosteric sea level (HSL) for 2018 minus 2016 over (a) 0–2000 dbar, (b) 100–500 dbar, (c) 0–100 dbar and (d) 500–2000 dbar. Contour lines (see inline numbers for TSL intervals) are also shown. In each panel, white shading indicates areas where bathymetry is shallower than each pressure reference level.

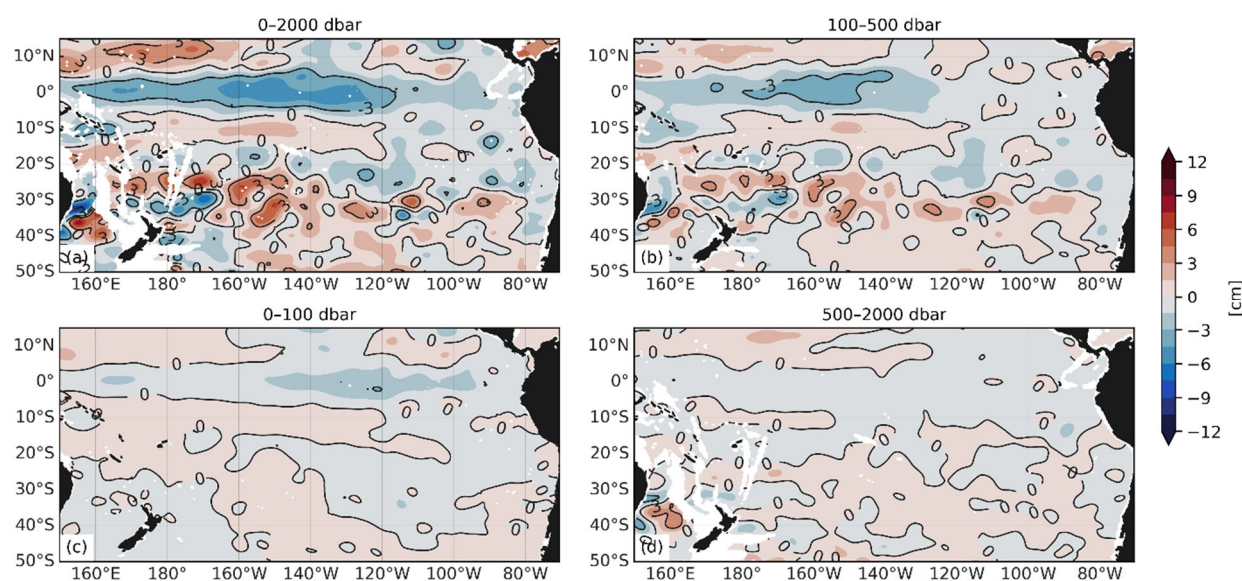


Figure S7. Differences in the 8th version of the In Situ Analysis System (ISAS20) Argo-based thermosteric sea level (TSL) for 2020 minus 2018 over (a) 0–2000 dbar, (b) 100–500 dbar, (c) 0–100 dbar and (d) 500–2000 dbar. Contour lines (see inline numbers for TSL intervals) are also shown. In each panel, white shading indicates areas where bathymetry is shallower than each pressure reference level.

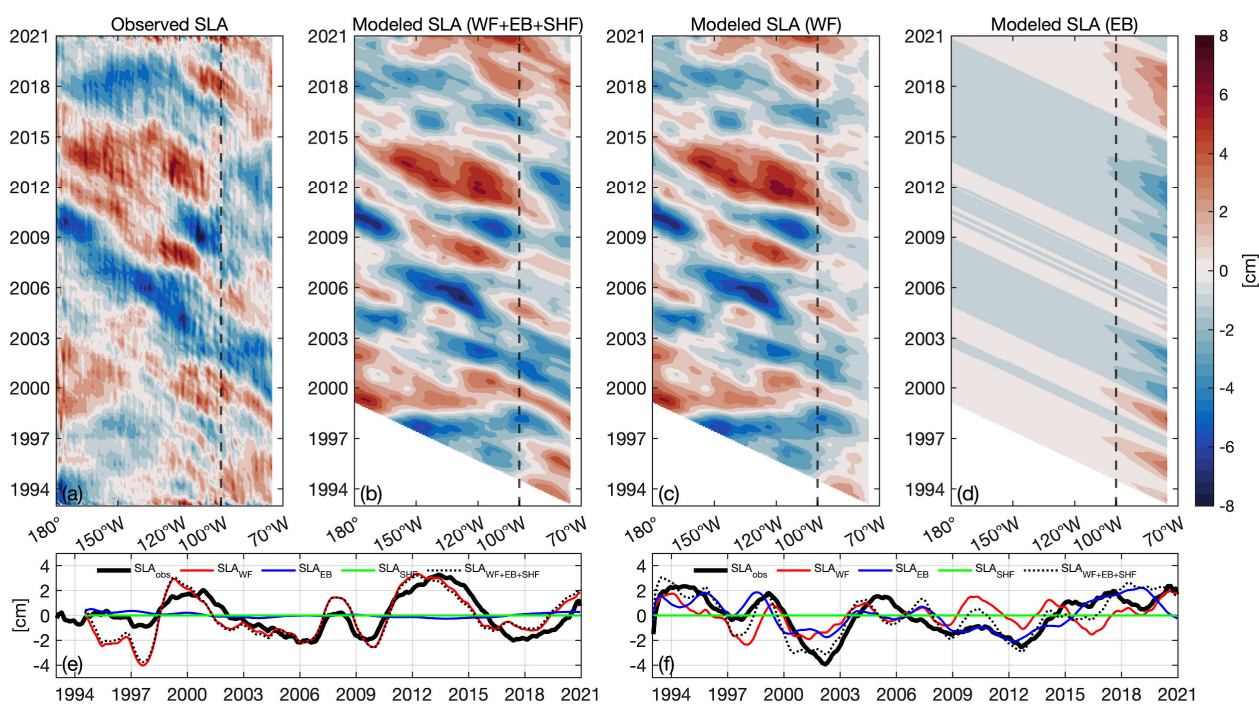


Figure S8. Same as Figure 9, but for the period starting from the beginning of the satellite altimetry era, 1993 to 2020.

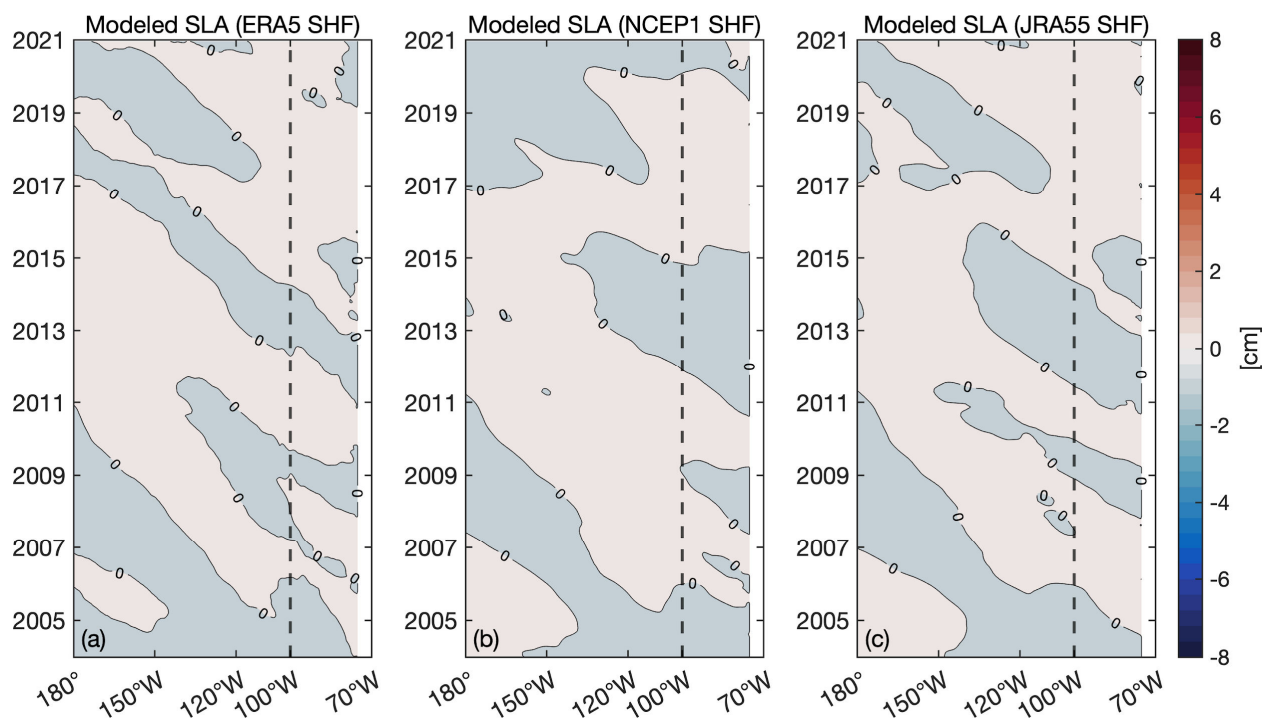


Figure S9. (a–c) Time-Longitude diagrams of interannual sea level anomaly (averaged over 34°S–36°S from 180° to 75°W) during 2004–2020 due to net surface heat forcing (SHF) only. Modeled SLA considering the SHF derived from (a) ERA5 (b) NCEP1 and (c) JRA55.